JCRS

Journal of Chemical Reactivity and Synthesis 2022: 12(3) 163-187

Research Article

Deletion of Auramine O and Crystal Violet from Industrial Aqueous Solution on to Albizia Lebbeck Leaves-Capped Silver Nanoparticles Synthesis Investigating Parameters Equilibrium

Fatemah Maghami[1], Maryam Abrishamkar[2*]

[1]Department of Chemistry, Islamic Azad University, Omidiyeh Branch, Omidiyeh, Iran & Research laboratory of Basic Science Department, Rafsanjani University Complex, Islamic Azad University Central Tehran Branch, Tehran, Iran

[2]Department of Chemistry, Ahvaz branch, Islamic Azad University, Ahvaz, Iran

ARTICLE INFO:

Received:
7 July 2022

Accepted:
14 September 2022

Available online:
23 September 2022

✉: M. Abrishamkar
maryam_abrishamkar@yahoo.com

ABSTRACT

The applicability of Albizia Lebbeck Leaves-capped silver nanoparticles (ALL-AgNPs) synthesis to dyes removal from aqueous solutions has been reported. The main goal of this work was development of a practical system to acquire the optimal conditions of removal accompanied by ultrasonic for maximizeing removal of Auramine O (AO) and Crystal Violet (CV) onto ALL-AgNPs in aqueous solution based on RSM (response surface methodology). To characterization of this novel materials techniques of X-ray diffraction (XRD), Fourier transform infrared (FT-IR) and scanning electron microscopy (SEM) were employed. The influences of several parameters including initial AO concentration (X1), initial CV concentration (X2), pH (X3), adsorbent dosage (X4), sonication time (X5) evaluated based on CCD (central composite design) using RSM. The process was empirically modeled to reveal the significant variables and their possible interactions. The optimal prameters of ultrasound time, pH, adsorbent mass, AO and CV concentration were obtained 5 min, 6.0, 0.025 g, 25 mg L-1, respectively. The application of isotherms in obtaining the thermodynamic parameters like enthalpy (ΔH0), free energy (ΔG0) and entropy (ΔS0) for adsorption process were confirmed. The maximum monolayer capacities (Q max) of AO and CV were obtained 73.2 and 48.7 mg/g, respectively under optimal conditions.

Keywords: Adsorption, Auramine O; Crystal Violet; Albizia Lebbeck Leaves-capped silver nanoparticles; experimental Design

1. Introduction

In some industrial products, including plastics, dye stuffs, textile, rubber, leather, cosmetics and tanning, enormous amounts of pigments and synthetic dyes utilized [1]. Diffusion of a large amount (about 15%) of all dyes used into the wastewater usually are occurred in the dyeing process. Aquatics life is endangered as a result of discharge of colored textile wastewater into the environment without efficacious action. As well as, several days, particularly the reactive dyes are non-biodegradable and recalcitrant [2]. Dyes and colors prevent the diffusion light and so, caused to the generation of carcinogenic and mutagenesis dangers. These problems are needed the design and development of new methods to access the achieve safe and clean environments [3]. AO (4, 40-dimethylamino benzophenonimide), as well as its hydrochloride salt are employed in the industries of textile, food dye, leather and coloring paper [4]. International agency for research on cancer (IARC) announced between chemicals, AO and CV dyes because of bio-transformation to reactive materials in target organs of humans and rats have carcinogenicity effects [5]. CV compound as a typical cationic dye is a member of the triphenylmethane group and extensively employed in dyeing wools and cotton, coloring paper and semi-permanent hair colorant. CV may damage the body by inhalation, swallowing and dermal contact and also has been proved in humans to causes cancer cells and intense eye itching [6,7].

This modification can increase the surface area and the number of reactive sites and so, considerably enhance the percents removal (R%) and also, adsorption capacity (q_e). Ultrasound irradiation or sonochemical synthesis is a method to speed up the phenomenon of acoustic cavitation which include the bubbles creation and collapse, growth of bubbles by the diffusion of a pressure wave via a liquid [8]. Cavitation effect as secondary effect in ultrasound process including the nucleation, growth and transient collapse of tiny gas bubbles, caused an improvement the mass transfer by convection pathway. It is arises from

some physical phenomena such as shock or acoustic waves, micro-turbulence, micro-jets and micro-streaming without considerable varations in equilibrium specs in the adsorption process [9]. Among these phenomena, shock waves are capable to cause microscopic turbulence in surface films around nearby solid particles [10]. Acoustic flow is the motion of a liquid that is caused by a sound wave and can be thought to convert sound into kinetic energy [11]. Ultrasound method has been shown to be a useful tool to amplification the process of mass transfer and eliminating the affinity among the adsorbent and the adsorbent [12].

Nanotechnology is generally an attractive research area into the production of nanoparticles (NPs) by different shapes, sizes, dispersions, chemical compositions and conceivable applications for human society subjects [13]. The synthesis of various NPs such as silver, gold, iron and so on is one of the main goals in nanotechnology research [14]. Silver NPs (AgNPs) due to their environmental biological and physicochemical charachteristics, such as catalytic activity, optical, electronic and magnetic attributes are the most useful and exciting NPs in many fields including the agriculture, medicine and industries [15]. In general, NPs are made using a different of physicochemical procedures that are very costly and potentially dangerous for the environment and so can cause the different biological threats. Biosynthetic processes can produce NPs with the better-defined morphologies and sizes than some of the chemical and physical procedures [16]. The effective application of the adsorption process is mostly pertains to the physicochemical properties and also adsorbent charachteristics, which is anticipated to have high absorption capacity, recoverable and affordable. Presently, different developed adsorbents have been employed to removal of particular organic substances from water samples. For this purpose, magnetic NPs (MNPs) due to high adsorption capacity, high surface area and small diffusion resistance have been widely evaluated as a new adsorbents. For example, these NPs have been emplyed to

removing the chemical substances such as metals, gases, paints, and environmental pollutants [17]. The preference of green synthesis of NPs than other methods is owing to slow kinetics, evaluation of crystal growth, offering better utilization and being stable. Green synthesis, in comparison with other traditional and chemical NPs synthesis methods, has shown advancement [18]. In this method, the need for toxic chemicals has been omitted. As a bottom-up approach, in green synthesis of NPs, the focus is on reducing the main reaction. The usefulness of biogenic synthesis lies in the reduction of environmental impact [19].

In the present work, a novel adsorbent of ALL-AgNPs were prepared in a simple procedure and identified using FTIR, SEM and XRD analysis. In AO and CV deletion process, Via studying the experimental conditions of solution pH, contact time, initial concentrations of AO and CV, adsorbent dosage and removal percentage (R%) dyes, were evaluated and optimization was accomplished based on the CCD using RSM. The adsorption process of AO and CV dyes described by the pseudo-second-order model and Langmuir isotherm model was applied to description of the equilibrium data. Finaaly, the kinetic study of the adsorption process was depicted compliance with the pseudo-second-order kinetic model. The effectuality of ALL-AgNPs in the deleting of AO and CV dyes from wastewater was proven.

2. Experimental

2.1. Instrumentation

Experiments were performed by FT-IR (PerkinElmer BX from Germany) at room temperature, XRD (Aanalytical X'PertPro, Almelo), V-530 model UV-Vis spectrophotometer (Jasco Co. from Japan), KYKY-EM 3200 SEM (Hitachi Firm, China) to study the morphology of samples at an accelerating voltage of 26 kV, a Tecno-GAZ SPA ultrasonic system using heating system (Italy) at power of 130 and frequency of 60 Hz, the

Metrohm 728 model pH/Ion meter (Switzerland, Swiss) for pH measurement. Laboratory glasswares were put overnight in 10% nitric acid solution. To set the temperature, a NBE ultra thermostat (VEB Prufgerate - WerkMedingen, Germany) was utilized [20].

2.2. Reagents and materials

All reagents, silver nitrate ($AgNO_3$), sodium hydroxide, hydrochloric acid were provided from Merck Co. (Germany). The methanol, AO and CV dyes were also provided from Sigma Aldrich. The preparation of solutions was done using double distilled water.

2.3. Synthesis of ALL-AgNPs

Silver nanomaterials have a variety of applications and in different areas, from medical equipment to electronic devices or in paintings and coatings, in soaps and detergents were used with different sizes and shapes [21]. Thus, in enhancing silver nanomaterials use in mentioned applications knowing distinct physical, optical, and chemical properties of them are essential. From this perspective, in their synthesis, considering the ensuing details of the materials are crucial: 1-surface property, 2-size distribution, 3-apparent morphology, 4-particle composition, and 5-dissolution rate.

Based on the method in the literature, the preparation of ALL-AgNPs was done by the abatement of $AgNO_3$, applying as a modifier. In summary, in a reaction flask which contained $AgNO_3$ solution (90 ml, 0.1 mM), 10 ml of ALL (0.1 mM) solution was added and stirred vigorously. After 15 min, was poured into the above solution at ambient temperature and stirred for 1h. Figure inset of UV–Vis spectrum of ALL-AgNPs was provided. The formation of ALL-AgNPs was proven by changing the color of the colloidal solution from dark to bright yellow. To guarantee the stability of the ALL-AgNPs solution for several weeks.

2.4. Adsorption experiments

The pH of solutions in the CCD experiments were adjusted by concentrated solutions of NaOH and HCl and various concentrations of AO and CV dyes into the erlenmeyer flasks (50 ml) were blended by certain values of the adsorbent at room temperature at fixed time in an ultrasonic bath. The sample solutions after adsorption process time, were instantly centrifuged. Then. the clear solutions were separated from the residual and determined using UV-Vis spectrophotometer [22]. The R% of AO and CVdyes and also, adsorption capacity (q_e) in mg g^{-1} were calculated based on the averages of repeated tests from the following equations:

$$R\% = \frac{C_{0i} - C_{ei}}{C_{0i}} \times 100 \quad (1)$$

$$q_i = \frac{V(C_{0i} - C_{ei})}{M} \times 100 \quad (2)$$

where C_{0i}, C_{ei}, V and M are the initial and equilibrium concentrations of dyes in aqueous solution in mg L^{-1}, the volume of the dyes solution in ml, the weight of the dried adsorbent in g [23].

2.5. Ultrasound assisted procedure

The AO and CV dyes removal was performed based on the ultrasound assisted procedure to adsorption prcess using ALL-AgNPs. The adsorption experiments based on sonochemical were accomplished in a batch mode with 0.025 g adsorbent in 50 ml solution of 25 $mg.L^{-1}$ AO and 20 $mg.L^{-1}$ CV dyes in pH= 6.0 for 5 min at the 25 °C. The dilute phase was examined to measuring concentrations of dyes by UV–Vis spectrophotometer.

2.6. CCD method

Run	X1	X2	X3	X4	X5	R $\%_{AO}$	R $\%_{CV}$

To decrease the number of tests and also the cost of these, evaluation the effective factors by designing experimental runs the CCD method was employed to optimization modeling. The factors of AO and CV concentrations, pH, amount of adsorbent and contact time were analysed which considered as X_1, X_2, X_3, X_4 and X_5, respectively. The R% values for these factors as independent parameters were calculated, which set at five levels (Table 1). To investigate the significance and acceptability the offered model, the analysis of variance (ANOVA) was studied using evaluation the lack of fit test, R-squared values (R^2) and Fisher test value (F-value). Finally, the mathematical relations among the independent pvariables of X_1, X_2, X_3, X_4 and X_5 were acquired with a second-order polynomial regression equation [24].

Table 1: Experimental factors, levels, and matrix of CCD.

Factors	levels			Star point$\alpha = 2.0$	
	Low (-1)	Central (0)	High(+1)	-α	+α
(X_1) AO Concentration (mg L^{-1})	10	15	20	5	25
(X_2) CV Concentration (mg L^{-1})	10	15	20	5	25
(X_3) pH	5.0	6.0	7.0	4.0	8.0
(X_4) Adsorbent mass (g)	0.0150	0.025	0.0350	0.005	0.045
(X_5) Sonication time (min)	2.0	4.0	5.0	2.0	6.0

1	10	20	7	0.035	2	98	100
2	15	15	4	0.025	4	95	95
3	20	20	7	0.035	6	97.9	99.4
4	25	15	6	0.025	4	98	100
5	15	15	6	0.025	4	94.45	94.87
6	10	10	7	0.015	2	88	88
7	10	10	7	0.035	6	100	100
8	15	15	8	0.025	4	97.5	95.77
9	15	15	6	0.025	4	95	95
10	15	15	6	0.025	4	94.7	95
11	20	10	7	0.015	6	95	95
12	10	10	5	0.035	2	100	100
13	15	15	6	0.025	4	95	95
14	15	5	6	0.025	4	97	99
15	10	20	5	0.035	6	100	100
16	15	15	6	0.025	4	95	95
17	20	20	5	0.015	6	73	81.8
18	15	15	6	0.005	4	70	78.8
19	20	10	5	0.015	2	80	96.47
20	20	10	7	0.035	2	99.69	100
21	10	20	5	0.015	2	88.5	90
22	20	20	5	0.035	2	100	98.45
23	15	25	6	0.025	4	95	95
24	15	15	6	0.045	4	100	100
25	15	15	6	0.025	8	99.48	98.52
26	10	10	5	0.015	6	99.33	100
27	5	15	6	0.025	4	100	100
28	10	20	7	0.015	6	100	96
29	15	15	6	0.025	4	94.57	94.7
30	20	20	7	0.015	2	80	81.7
31	20	10	5	0.035	6	100	100
32	15	15	6	0.025	4	95	95

2.7. Desirability function

For each separate response, a function produced based on the desirability function (DF), which lead to the global function (D) as final output, which the maximum value supporting to achieving the optimal quantities [25]. The application and basis of DF process to the finest forecasting the actual treatment of the adsorption system have been pointed out already [26]. The favorable characteristics presented the anticipated levels of factors producing the most desired responses.

3- Results and discussion

3.1. Characterization and evaluation of the ALL-AgNPs

The isotherm of nitrogen adsorption–desorption at 77 K onto ALL-AgNPs is shown in Fig.1. The average of specific surface area and total pore volume of ALL-AgNPs based on the BET method results, were obtained 0.3 m^2/g and 3.77×10^{-3} cm^3/g, respectively. The amount of q_e of ALL-AgNPs controlled by chemical reactivity and porosity of surface functional groups. Having information about surface function groups increases the insight of q_e of the ALL-AgNPs.

The XRD pattern of the ALL-AgNPs as shown in Fig.2, represents a peak at 38.5 (122), 45.0 (111), 52.2 (200), 54.4 (231) and 72.7 (220) confirmed the reflections and diffractions of the carbon atoms [27]. As observed, the highly crystalline type of the formation phases after functionalization by activated carbon produced from ALLs was corroborated, while the great peak intensity at 45.0 (111) presented excisting a small value of substance in the amorphous form. The results of XRD pattern depicted the activated carbon were obtained from ALL-AgNPs.

Because the heavy metal ions removal occurred usually using complexation or electrostatic attraction between the metal ions and different functional groups, therefore evaluation the functional groups is very momentous [28]. The FTIR spectrum of activated carbon produced

from ALL-AgNPs in Fig.3 indicated the absorption band about 3451 cm^{-1} that corroborated the attendance of O-H functional groups in the phenolic or alcoholic structures. The absorption bands at 3101 and 2158 cm^{-1} indicated the presence of C-H and C=O functional groups, respectively. Also, the band at 776.8 cm^{-1} was related to the Ag-O groups in the ALL-AgNPs structure.

Fig.4 shows the SEM analysis to evaluation the morphology propertied of the samples. ALL-AgNPs were illustrated the homogeneous, smooth and ordered with uniformity in size distribution. Following modification of the surface with activated carbon produced from ALL-AgNPs, NPs with rough, larger, and bundled were obtained [29].

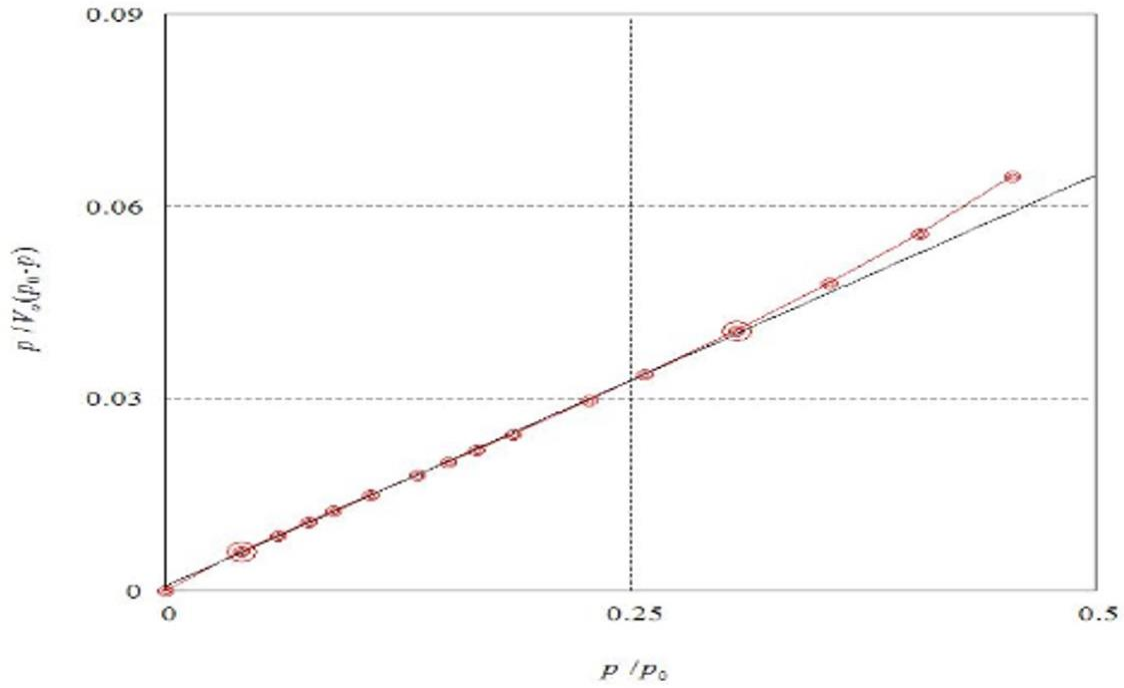

Fig. 1 : The BET image of the fabricated ALL-Ag NPs.

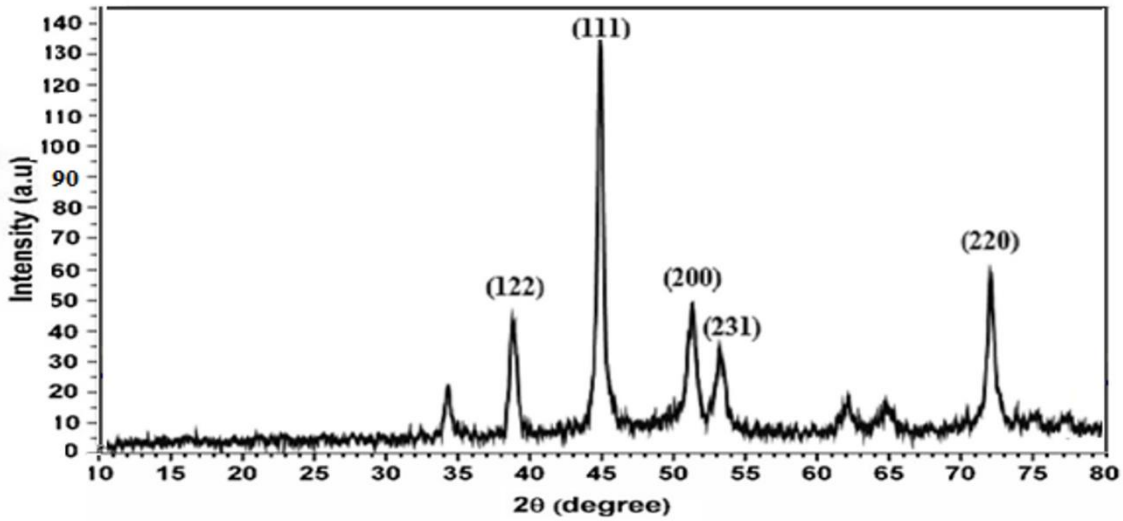

Fig. 2 : The XRD image of the fabricated ALL-AgNPs.

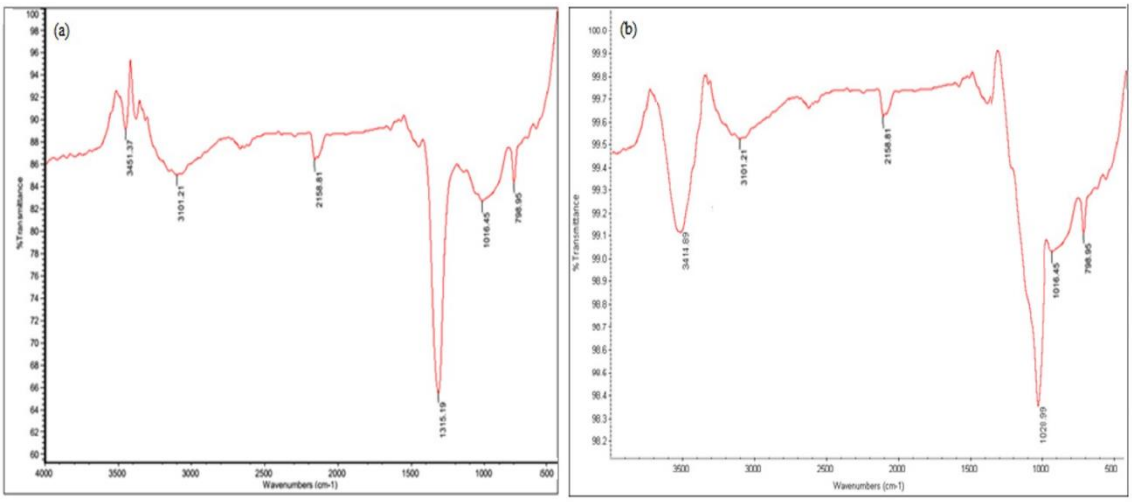

Fig. 3: (a) FTIR spectra of the prepared Albizia Lebbeck Leaves of active carbon, (b) FTIR spectra of the fabricated ALL-AgNPs.

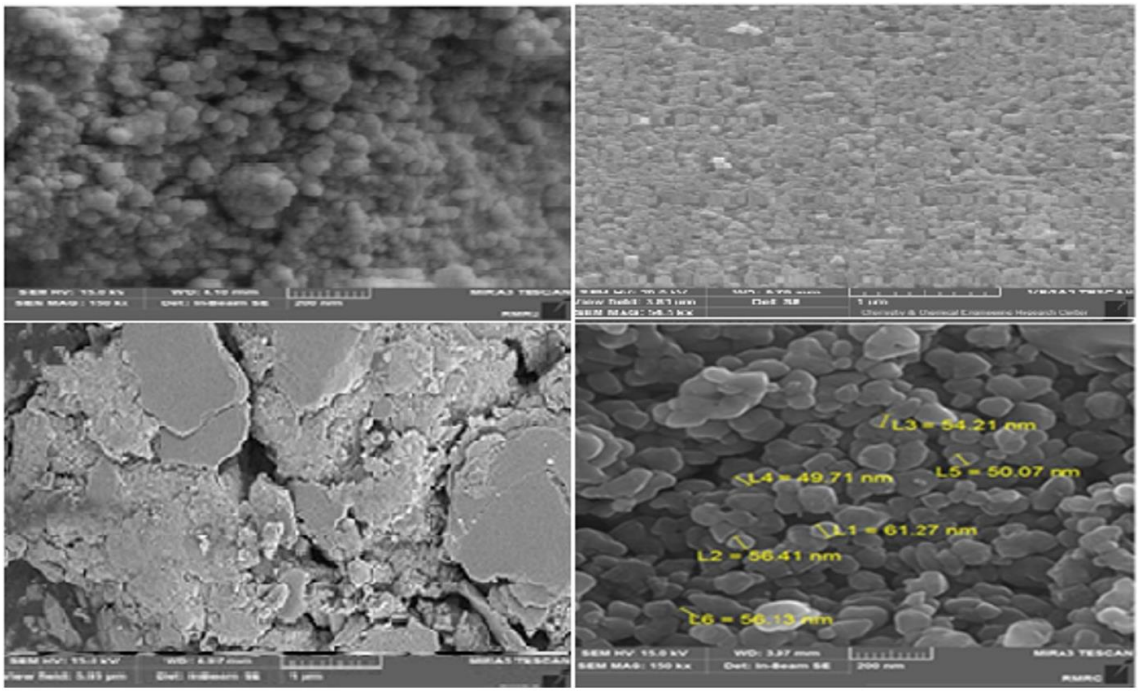

Fig. 4: The (SEM) image of the ALL-AgNPs.

3.2. Modeling the process and statistical analysis

CCD was performed using RSM to forming a systematic series of tests based on the 50 runs in five levels. The RSM method creats a way to nonlinearly model for evaluation of investigational data [30]. The CCD avoids performing inessential tests and assists to evaluate the synergies between the parameters. Another way of saying that, analysis of the interaction among the variables the with CCD using RSM method was easily performed. In the CCD the variables of X1 (initial concentration of AO), X2 (CV concentration), X3 (pH), X4 (adsorbent dosage) and X5 (sonication time), which may make the changes in R% amounts of AO and CV as a response. A good fit was obtained in the graphs of experimental R% vs. calculated R% by equation. The encoded amounts for the quadratic equations after elimination the unimportant terms are depicted in Eq. (1). Already, about the CCD using RSM, the detailed comments has been introduced [31,32]. Table 2 illustrated the ANOVA to characterize the importance level of each variable. The importance of each parameter was

investigated by the corresponding F- and p-values. In the ANOVA table, a p-value less than 0.05 illustrates the statistical importance of a variable at a confidence level of 95%. The DF process was applied to investigate the optimal conditions based on Derringer's desirability function.

$$R\%_{AO}=95.709-2.1767X_1 -1.0258X_2+0.94833X_3+6.3233X_4+2.0955X_5-1.4350X_1X_2+1.3388X_1X_3+2.9638X_1X_4-1.1638X_1X_5+0.69000X_2X_3+1.0650X_2X_4-1.3900X_2X_5-1.6612X_3X_4+1.4612X_3X_5-1.9138X_4X_5+0.66726X_1^2+0.91726X_2^2-0.020244X_3^2-2.8327X_4^2-0.41595X_5^2 \quad (1)$$

$$R\%_{CV}=95.775-0.88250X_1-1.3383X_2-0.21167X_3+4.6367X_4+1.2054X_5-1.7575X_1X_2+0.33625X_1X_3+1.0550X_1X_4-1.1513X_1X_5+1.2700X_2X_3+1.7388X_2X_4-0.21750X_2X_5+0.53250X_3X_4+1.4887X_3X_5-0.98000X_4X_5+0.94960X_1^2+0.94960X_2^2-0.20415X_3^2-1.7004X_4^2-0.12982X_5^2 \quad (2)$$

The P-values of the lack of fits corresponding values of AO and CV, using ANOVA of $R\%_{AO}$ and R% CV were acquired 0.11 and 0.30, respectively. These values demonstrate the application of the anticipative models. The adjusted R^2 and R^2 values were obtained close to 1 for both models, which corroborated the goodness of the fit of a statistical model. As it is seen, the pH factor and its interaction of this with concentrations of AO and CV based on eq.(3) are considerable,which have a negative effect on R% AO. The adsorbent amounts as an other significant factor depicted positive effect R% AO.

Table 2: Analysis of variance (ANOVA) for R% of AO and CV.

Source of variation	Df	AO				CV			
		Sum of square	Mean square	F-value	P-value	Sum of square	Mean square	F-value	P-value
Model	20	3014	150.7	22.78	< 0.0001	977.95	48.898	8.4833	0.000412
X_1	1	153.8	153.8	23.26	0.00053	18.691	18.691	3.2428	0.099187
X_2	1	739.9	739.9	111.9	< 0.0001	42.987	42.987	7.4579	0.019546
X_3	1	1243.0	1243.0	187.9	< 0.0001	1.0753	1.0753	0.18655	0.67415
X_4	1	13.89	13.89	2.111	0.1752	515.97	515.97	89.516	< 0.0001
X_5	1	32.16	32.16	4.863	0.0497	24.653	24.653	4.277	0.062979
X_1X_2	1	32.43	32.43	4.9003	0.0488	49.421	49.421	8.5741	0.013736
X_1X_3	1	22.09	22.09	3.341	0.0949	1.809	1.809	0.31385	0.58655

X_1X_4	1	171.1	171.1	25. 89	0.0003	17.808	17.808	3.0896	0.10655
X_1X_5	1	62.25	62.25	9.411	0.0107	21.206	21.206	3.6791	0.081416
X_2X_3	1	13.47	13.47	2.036	0.1813	25.806	25.806	4.4772	0.057977
X_2X_4	1	39.56	39.56	5.981	0.0325	48.372	48.372	8.3921	0.014525
X_2X_5	1	2.756	2.756	0.417	0.5319	0.7569	0.7569	0.13132	0.72394
X_3X_4	1	87.89	87.89	13.29	0.0039	4.5369	4.5369	0.78711	0.39396
X_3X_5	1	190.3	190.3	28.77	0.0002	35.462	35.462	6.1524	0.030552
X_4X_5	1	21.76	21.76	3.290	0.0970	15.366	15.366	2.6659	0.13079
X_1^2	1	91.93	91.93	13.91	0.0030	26.291	26.291	4.5613	0.056021
X_2^2	1	24.64	24.64	3.726	0.0798	26.291	26.291	4.5613	0.056021
X_3^2	1	62.34	62.34	9.425	0.0107	1.2151	1.2151	0.21081	0.65508
X_4^2	1	50.37	50.37	7.615	0.0186	84.299	84.299	14.625	0.002822
X_5^2	1	8.328	8.328	1.259	0.2852	0.28347	0.28347	0.049179	0.82856
Residual	11	72.76	6.614			63.404	5.764		
Lack of Fit	5	44.07	7.345	1.280	0.4021	41.28	8.2561	2.2391	0.17741
Pure Error	6	28.68	5.737			22.123	3.6872		0.000412
Cor Total	31	3086				1041.4			0.099187

3.3. RSM graphs

The 3D RSM graphs dependent on R% of dyes were obtained with consideration of optimal the main parameters for gaining effective data concerning the conceivable interaction between parameters. Based on the Eqs. of (5) and (6) and also, as shown in Figs. 5 and 6, the results of the main interactions of the variables on the curvature of the surfaces are detected as anticipated. Fig. 5 and 6 illustrated the RSM graph based on the R% changes of dyes vs. the adsorbent mass. As it is seen, with increasing adsorbent dosage, the R% of dyes was depicted positive increase. At lower dosages of ALL-AgNPs due to the higher ratio of dye molecules to the unoccupied sites of the adsorbent, R% amounts were considerably decreased. As observed, the highest absorption of AO dye can be obtained in a short ultrasound time, which potently assists the large sharing of power ultrasound in mass transfer

and therefore, the higher absorption efficiency of AO dye. The interaction of pH with initial concentrations of AO and CV depicted in Figs. 6a and 6b, respectively. The negative relation between the pH and R% was achieved and at greater pH values, R% values were decreased. At lower pH values, the protonation of functional groups in the adsorbent structure leads to the production of a positive charge on the adsorbent surface. Therefore, the strong forces were achieved between the adsorbent surface and cationic dye molecules and so, R% amounts were increased. Based on the results of the effect of ultrasound time in Fig. 6c depicted with increasing ultrasound time, the CV dye adsorption was increased.

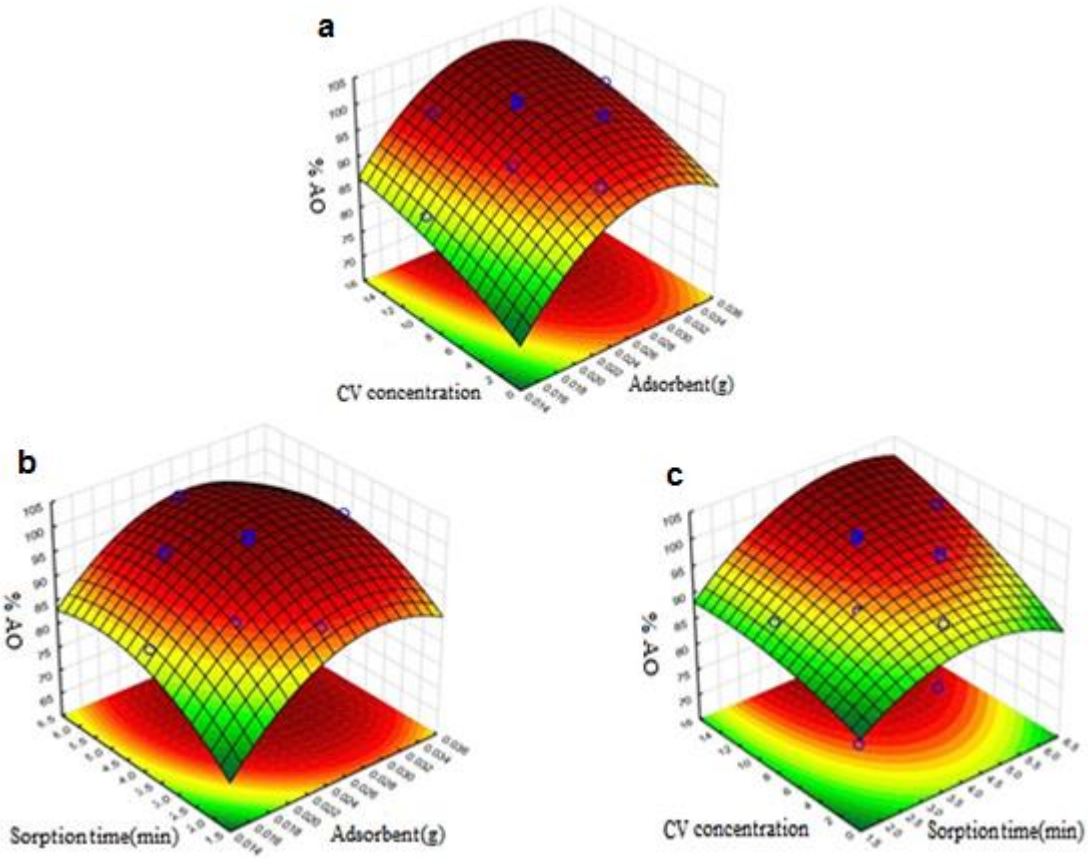

Fig. 5: RSM plots of AO removal: (a) initial concentration of AO vs. adsorbent dosage (b) sorption time vs adsorbent dosage (c) initial concentration of AO vs. sorption time

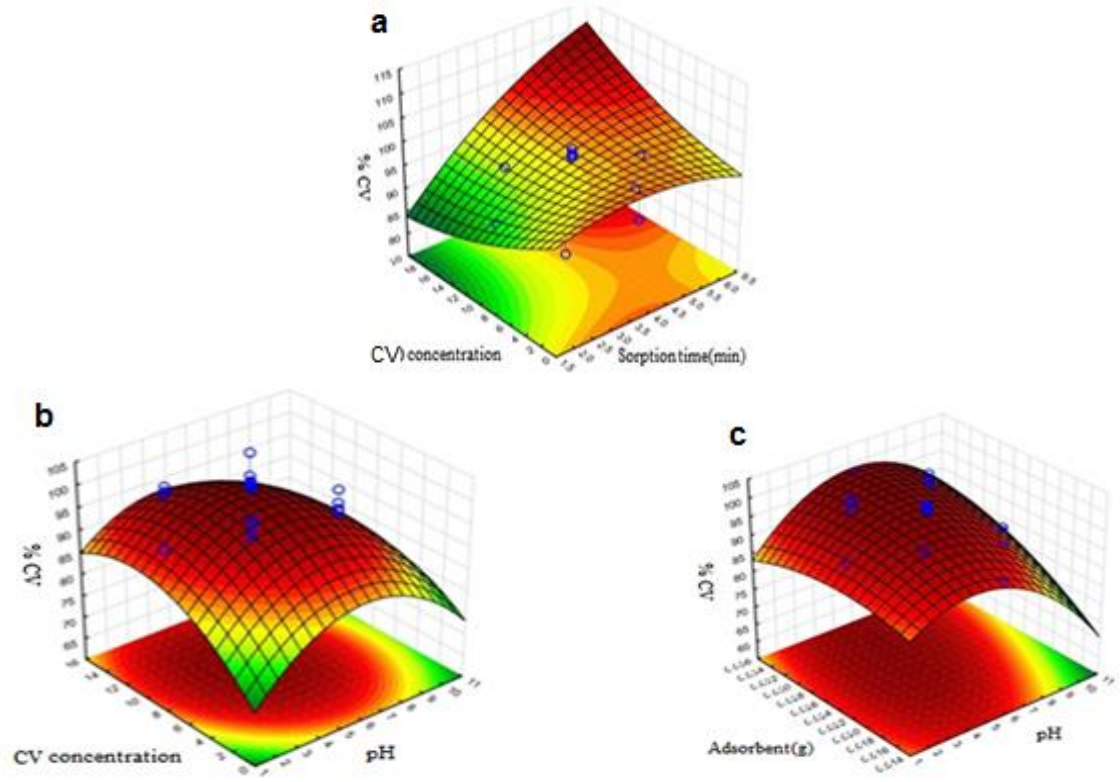

Fig. 6 : RSM plots of CV removal: (a) initial concentration of CV vs. sorption time, (b) initial concentration of CV vs. pH (c) adsorbent dosage vs. pH

3.4. CCD optimization using DF

The characteristics of the desired choices with the predicted amounts in STATISTICA software (V. 10.0) were employed to optimize the process (Figure 7). The utility in the range of 0.0 (unfavorable) to 1.0 (very desirable) was applied to acquiring a final output (universal function or D) which is the basis of optimization process. The matrix results in CCD experiments for CV and AO were acquired as minimum (70% and 78.8%) and maximum (100 % and 100%), respectively. Based on the obtained values, to each of dependent parameters with R%, the DF settings were acquired and illustrated in the right-hand side of Fig. 7. The desirabile conditions were determined 0.0, 0.5 and 1.0 for minimum, middle and maximum removal conditions as (70% and 78.8%), (85% and 89.4%) and (100% and 100%) for CV and AO dyes, respectively.

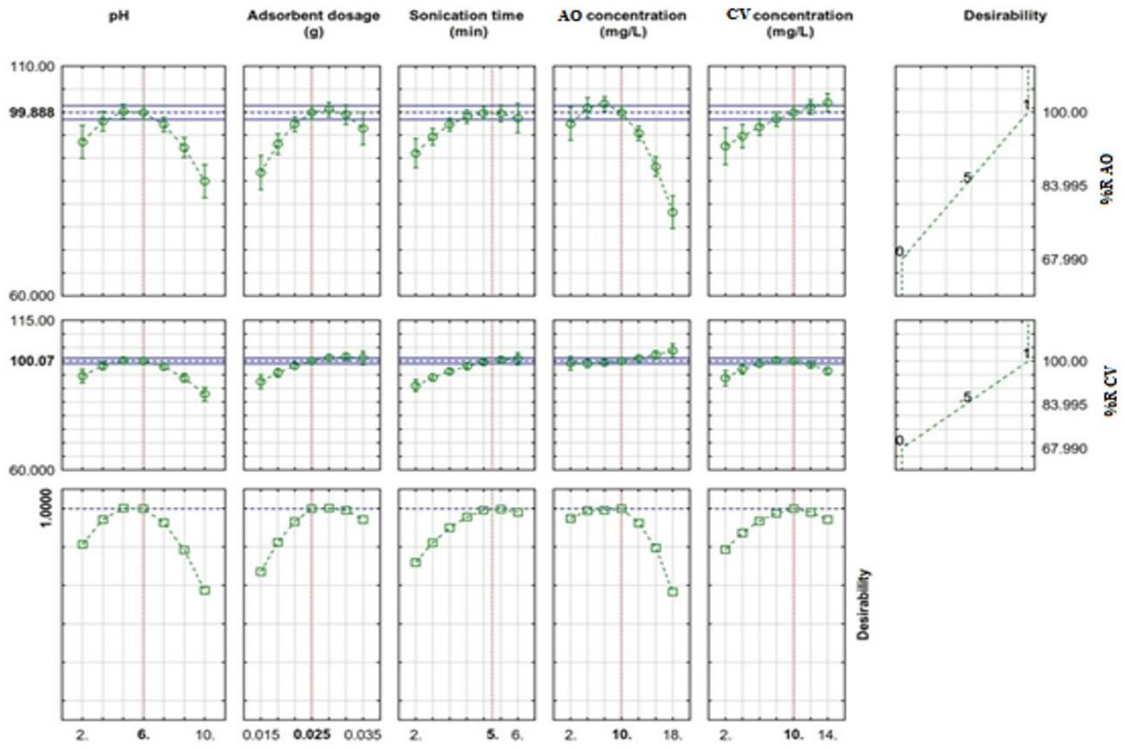

Fig. 7: The predicated values profiles and desirability function to R% of AO and CV. The current values after optimization shows with dashed lines.

3.5. Biosorption isotherms

The distribution of portion of dye molecules among solid and liquid phases at equilibrium was escribed by adsorption isotherm. With the help of four adsorption model isotherms of Freundlich, Langmuir, Dubinin-Radushkevich and Temkin models, adsorption of AO and CV dyes onto ALL-AgNPs was displayed [33].

3.6. Adsorption equilibrium investigation

Accurate plotting of the adsorption equilibrium isotherm depends on mathematical relationship between the adsorbed amounts of species (qe) as mg g^{-1} and the equilibrium non-adsorbed amounts of species (C_e) in solution as mg L^{-1} at specific temperature [34,35]. To characterize the isotherm of adsorption process, the Langmuir, Freundlich, and Dubinin–Radushkevich (D-R) model isotherms were employed.

1) The Langmuir isotherm model to investigate the adsorbent surface as homogeneous distribution with identical sites and no interaction existed amongst adsorbed molecules applied as the following equation [36]:

$C_e/q_e = 1/K_L q_{max} + C_e/q_{max}$

In the above equation C_e, q_e, q_{max}, K_L refers to the equilibrium concentration (mg L^{-1}), adsorption capacity in the aqueous solution (mg g^{-1}), and the maximum adsorption capacity of the adsorbents in the aqueous solution (mg g^{-1}), Langmuir constant (L/mg). Due to the higher correlation coefficient in all adsorbent dosages, the Langmuir was demonstrate as the best model. The rise in the quantity of sorbent led to a remarkable boost in the quantity of adsorbed ions.

In Freundlich isotherm model the calculation the parameters of the adsorption intensity (n) and Freundlich constant (K_F) were done using the slope and intercept of the linear plot of $\ln q_e$ vs. $\ln C_e$.

Temkin model was employed to evaluation of the interaction between adsorbent and adsorbate and also calculation of the heat of adsorption process. In these model, the parameters of T, t, R, B, and K refer to stands for the absolute temperature (K), heat of the adsorption (J/mol), universal gas constant (8.314J/mol.K), Temkin constant, the equilibrium binding constant (L/mg).

The D–R model was employed to estimating the apparent free energy, porosity and the adsorption properties [37]. By fitting these models with the experimental results and due to the higher R^2 values (0.97 – 0.99) for AO and CV dyes (Table 3), the Langmuir isotherm was selected the best model to illustrate the adsorption process of dyes at the surface of ALL-AgNPs, that depicted the a monolayer of adsorbate profuction on the surface of the ALL-AgNPs. As well as, the equilibrium distribution of dyes between the liquid and solid phases was specified with this model.

Table 3: Various isotherm constants and their correlation coefficients calculated for the adsorption of AO and CV onto ALL-AgNPs.

Isotherm	Equation	parameters	Value of parameters for AO	Value of parameters for CV
Langmuir	$q_e=q_m bC_e/(1+bC_e)$	Q_m(mg/g)	70/3	48/48
		K_a (L/mg)	1/491	1/344
		R^2	0/99	0/97
Freundlich	$\ln q_e = \ln K_F + (1/n) \ln C_e$	1/n	3/81	3/96
		K_F (L/mg)	9/44	4/67
		R^2	0/96	0/93
Tempkin	$q_e = B_1 \ln K_T + B_1 \ln C_e$	B_1	15/55	10/63
		K_T (L/mg)	10/675	9/3
		R^2	0/98	0/94
Dubinin-Radushkevich (DR)	$\ln q_e = \ln Q_s - B\varepsilon^2$	Q_s (mg/g)	60/35	29/135
		B	6E-07	5E-07
		E (kj/mol)	8535.53	3354.1
		R^2	0/97	0/93

3.7. The kinetic study of adsorption

Values of the kinetic parameters the models of pseudo-first- and pseudo-second order [33] are presented in Table 4 along with $q_{e,\,cal}$, $q_{e,\,exp}$ and R^2. The R^2 value of 0.999-0.999 obtained for AO and CV dyes adsorption onto ALL-AgNPs based on the pseudo-second-order equation. Also, the value $q_{e,cal}$ depicted a very good agreement with the obtained experimental results. This observation was strongly confirmed the adsorption of AO and CV dyes onto ALL-AgNPs with a pseudo-second-order process. The closer the value of R^2 to unity depicted a optimum best-fit values due to the film diffusion model. Since the straight lines did not cross the origin, so indicated the resistance or film diffusion may only rate-limiting step. Based on the of q_t v lnt plots, the Elovich constants can calculate [35]. The lower values of R^2 revealed the inappropriate of this model to AO and CV dyes adsorption onto ALL-AgNPs adsorbents (Table 4).

Table 4: Various Kinetic constants and their correlation coefficients calculated for the adsorption of AO and CV onto Albizia Lebbeck Leaves-capped Ag NPs nanoparticles.

Model	parameters	Value of parameters for AO	Value of parameters for CV
pseudo-First-order kinetic	$k_1(min^{-1})$	0.626	0.57
	qe (calc) (mg/g)	2.71	1.48
	R^2	0.958	0.95
pseudo-Second-order kinetic	k_2 (min^{-1})	0.042	0.067
	q_e(calc) (mg/g)	20.24	22.93
	R^2	0.999	0.999
Intraparticle diffusion	K_{diff} (mg g-1 min-1/2)	1.31	4.77
	C (mg/g)	17.07	10.13
	R^2	0.94	0.97
Elovich	β (g/mg)	1.05	0.28
	α (mg g-1 min-1)	222.5	219.0
	R^2	0.94	0.98
q_e(exp) (mg g^{-1})		50.40	33.77

3.8. Adsorption thermodynamics

In the adsorption processes the ΔG°, ΔH° and ΔS° are theGibbs free energy change, enthalpy change and entropy change as the thermodynamic parameters were characterized based on the following equations [36]:

$$\Delta G^{\circ} = -RT \ln K_{ad}$$

$$\ln K_{ad} \frac{\Delta H^{\circ}}{RT} + \frac{\Delta S^{\circ}}{R}$$

ΔG can be obtained from the slope of lnKe vs. 1/T graph. In Table.5, the brief of the thermodynamic parameter results of AO and CV dyes adsorption onto derived ALL-AgNPs at different temperatures is shown.

By employing the adsorption eq. of AO and CV dyes, the ΔG^o values were computed. In Table.5, the exothermicity nature of the process was apparent since by increasing in the temperature between 298 and 348 K, ALL-AgNPs was decreased and hence the nature of exothermicity to adsorption process was accepted. The thermodynamic variables amounts in Table 5 were computed using the plots [36]. Possibility and spontaneous behavior the nature of the adsorption process was demonstrated with a negative value for GU. On the other hand, the exothermicity behavior adsorption process was confirmed by the negative values of ΔH^o and ΔS^o which indicatioed the randomness change at the derived ALL-AgNPs solution interface during the sorption. The values of ΔG^o up to -1.1697 kJ/mol for AO and -0.9257 kJ/mol for CV dyes were confirmed the physical adsorption or electrostatic interaction between the dyes and sorption sites. The acquired values of ΔG^o for AO and CV dyes are <-5 kJ/mol revealed the dominance of the physical mechanism in the adsorption process [38].

Table 5: The thermodynamic parameters for the adsorption of AO and CV dyes onto Albizia Lebbeck Leaves-capped Ag NPs nanoparticles adsorbent.

Dyes (mg/L)	T (^{O}K)	Kc	value of ΔS^o (J/mol K)	value of ΔH^o(J/mol)	value of ΔG^o(J/mol)
Auramine O (AO) dye	288	132	-273.7	-76.917	-11697/6
	308	165.25			-13085/1
	318	220/66			-14274/7
	328	331/5			-15833/7
	338	1329			-20213
Crystal Violet (CV) dye	288	47/66	-131.49	-29.24	-9257/46
	308	57/4			-1٠376
	318	96/33			-12٠82.3
	328	145			-13577/7
	338	291			-15940/5

4. Conclusions

The synthesis of ALL-AgNPs as adsorbent has been carried out and potency of this

adsorbent to AO and CV dyes removal from aqueous solutions has been investigated. The evaluations were designed based on RSM, and the quadratic model was applied to prognosis the parameters. The effect of parameters (concentration of AO and CV dyes, pH, adsorbent dosages and contact time) on adsorption of AO and (CV) dyes was evaluated with CCD using RSM design. The dyes adsorption onto ALL-AgNPs was found to be 99.2% at pH = 6.0, 25.0 mg L^{-1} for concentration of AO and CV dyes, adsorbent mass of 0.025 …….. and sonication time of 5.0 min. At optimal conditions, the experimental R% of ALL-AgNPs reached. (R^2= 0.99-0.97) for AO and CV dyes. Different isotherm models (Langmuir, Freundlich, D-R and Temkin) have been examined for the adsorption process, but it became apparent that the Langmuir model could successfully describe the equilibrium data. The maximum (Qm) value of 73.2 mg/g for AO and 48.7 mg/g for CV dyes. The adsorption kinetic was specified obey the pseudo-second-order model. In addition, the possibility of recycling the adsorbent was well proved by desorption studies. Based on the results from the linear regression-based analysis, it was revealed that the derived empirical models represented a passable prediction of performance onto ALL-AgNPs with significant determination coefficients AO and CV dyes (R^2= 0.999-0.999). Additionally, At the temperatures under investigation, spontaneous adsorption of AO and CV dyes was reported. Also, the endothermicity of the process of adsorption was corroborated by the negative values of ΔG^o, $\Delta H^{o,}$ and ΔS^o. The study aimed at developing low-cost, highly available, and powerful of AO and CV dyes adsorbents from natural wastes for the replacement of existing commercial adsorbents. ALL-AgNPs, in comparison with other adsorbents, show a high values of q_e for AO and CV dyes deletion from aqueous medium.

References:

[1] S. Bagheri, H. Aghaei, M. Monajjemi, M. Ghaedi, K. Zare. Eurasian *J Anal Chem.*13 (3) (2018) 1-10.

[2] Z. Rahmani, M. Kermani, M. Gholami, A. J. Jafari, N. M. Mahmoodi, *Iran J Environ Heal Sci Eng*.9(1) (2012) 14-25.

[3] A. Martelli, F. Mattioli , E. Merreto, G. Brambilla Campart, D. Sini, G. Bergamaschi, G. Brambila, *Toxicology* 130 (1998) 29-41.

[4] A. Asfaram, M. Ghaedi, S. Agarwal, I. Tyagib, V. K. Guptab. *RSC Adv.* 5 (2015) 18438-18450.

[5] .R. Martins, J.A.V Rodrigues, O.F.H Adarme, T.M.S. Melo, L.V.A. Gurgel, L.F. Gil, *J Colloid Interface Sci* , 494 (2017) 223-241.

[6] A. Saeed, M. Sharif, M. Iqbal. *J Hazard Mater* ,179 (2010) 564-572.

[7] Y. Lin,X. He,G. Han,Q. Tian,W. Hu. *J Environ Sci,* 23(12) (2011) 2055-2062.

[8] G. Haghdoost. *J Phys Theor Chem.* 15 (2019) 141-148.

[9] O. Acisli ,A. Khataee ,S. Karaca ,M. Sheydaei, *Ultrason Sonochem* ,31 (2016) 116-121.

[10] S. Bagheri ,H. Aghaei ,M. Ghaedi ,A. Asfaram ,M. Monajemi ,A.A. Bazrafshan , *Ultrason Sonochem,* ,41 (2018) 279-287.

[11] M. H. Entezari, Z.S. Al-Hoseini, N. Ashraf, *Ultrason Sonochem* , 15(4) (2008) 433-437.

[12] M. Kiani,S. Bagheri, N. Karachi, E. Alipanahpour Dil , *Desalin Water Treat.* 152 (2019) 366-373.

[13] M. Namdari,B. Negahdari,A. Eatemadi. *PIET Nanobiotechnology*. 87 (2017) 209-222.

[14] S. Falahrodbari. *Orient J Chem.* 33(2) (2017) 910-919.

[15] M. Ghaedi, B. Sadeghian, A.A Pebdani, R. Sahraei , A. Daneshfar, *C. Duran. Chem Eng J*, 187 (2012) 133-141.

[16] A. D'Amico, G. Pennazza, M. Santonico,E. Martinelli, C. Roscioni, G. Galluccio , *Lung Cancer* ., 68(2) (2010) 170-176.

[17] Y.C. Sharma,V. Srivastava,V. K. Singh, S.N. Kaul, C. H. Weng, *Environ Technol.* 30(6) (2009) 583-609.

[18] IV International Conference „ECOLOGY OF URBAN AREAS 2014—, 9 -10th October 2014, Zrenjanin, Serbia. 2014. 9–10 p.

[19] H. Korbekandi,S. Iravani, S. Abbasi, *Crit Rev Biotechnol.* 29(4) (2009) 279-306.

[20] A. C. Burduşel,O. Gherasim,A. M. Grumezescu,L. Mogoantă,A. Ficai, E. Andronescu, *Nanomaterials*.8(9) (2018) 1-8.

[21] S. Justin Packia Jacob,J. S. Finub, A. Narayanan, *Colloids Surfaces B Biointerfaces.* 91(1) (2012) 212-214.

[22] W. P. Utoo1, E. Santoso, G. Yuhaneka,A. I. Triantini, M. R. Fatqi, M. F. Huda , *Journal Kimia*. 13(1) (2019) 104.115

[23] J. Ma, F. Yu,L. Zhou, L. Jin, M. Yang,J. Luan , *ACS Appl Mater Interfaces.* 4(11) (2012) 5749-5760.

[24] E. A. Dil, M. Ghaedi,A. Asfaram, A.A. Bazrafshan , *Ultrason Sonochem*. 46(2018) 99-105.

[25] H.S. Ghazi Mokri, N. Modirshahla, M.A.Behnajady, B. Vahid. *Int J Environ Sci Technol.* 12(4) (2015) 1401-1423.

[26] M. Dastkhoon, M. Ghaedi,A. Asfaram, M. H. Ahmadi Azqhandi, M.K. Purkait, *Chem Eng Res Des*124(2017) 222-237.

[27] F. Paquin, J. Rivnay, A.Salleo, N. Stingelin, C. Silva. *J Mater Chem C* , 3(2015) 10715-10722.

[28] C. Krishnaraj,E. G. Jagan, S. Rajasekar, P. Selvakumar,P. T. Kalaichelvan, N. Mohan. *Colloids Surfaces B Biointerfaces.* 76(1) (2010) 50-56.

[29] M. Ghaedi, A.Shahamiri, S.Hajati, B. Mirtamizdoust. *J Mol Liq.* 199(2014) 483-488.

[30] S. Kashefi, S. M. Borghei, N. M. Mahmoodi , *Prog Color Color Coatings.* 12(3) (2019) 179-190.

[31] M. Ghaemi, G. Absalan, L. Sheikhian , *J. Iran Chem. Soc.* 11(6) (2014) 1759-1766.

[32] A. Asfaram, M. Ghaedi,S. Hajati,M. Rezaeinejad,A. Goudarzi,M. K. Purkait, *J Taiwan Inst Chem Eng* 53 (2015) 80-91.

[33] M. T. Yagub, T. K. Sen, H. M. Ang, *Water Air Soil Pollut*. 223(8) (2012) 5267-5282.

[34] M. Nanoparticles. *Analytical and Bioanalytical Research*, 99 (2008) 66-78.

[35] S. Hajati,M. Ghaedi,H. Mazaheri , *Desalin Water Treat.* 57(7) (2016) 3179-3193.

[36] A. I.Adeogun, R. B. Balakrishnan, *Appl. Water.Scienc.* 7 (2017) 1711-1723.

[37] S. Hamid,P/ Davar, A. Manbohi, *Iran J Chem Chem Eng*. 35(1) (2016) 63-82.

[38] S. Afroze,T. K. Sen, M.Ang, H. Nishioka. *Desalin Water Treat.* 57(13) (2016) 5858-5892.